

# Nanoscale Suppression of Magnetization at Atomically Assembled Manganite Interfaces

J. J. Kavich,<sup>1,2</sup> M. P. Warusawithana,<sup>3</sup> J. W. Freeland,<sup>2</sup>  
P. Ryan,<sup>2</sup> X. Zhai,<sup>3</sup> R. H. Kodama,<sup>1</sup> and J. N. Eckstein<sup>3</sup>

<sup>1</sup>Department of Physics, University of Illinois at Chicago, Chicago, IL 60607

<sup>2</sup>Advanced Photon Source, Argonne National Laboratory, Argonne, IL 60439

<sup>3</sup>Department of Physics, University of Illinois at Urbana-Champaign, Urbana, IL 61801

(Dated: 13 November 2005)

## Abstract

We used polarized x-rays to probe the depth-dependent magnetic profile of a  $\text{La}_{1-x}\text{Sr}_x\text{MnO}_3$  (LSMO)/ $\text{SrTiO}_3$  (STO) and a modified LSMO/ $\text{LaMnO}_3$  (LMO)/STO interface. The electronic and magnetic structure of the LMO layer at the modified interface appears to be equivalent to the underlying LSMO film, and we show a larger FM moment in the LMO/STO interface than in the LSMO/STO interface at low temperature. For all temperatures, the magnetic profiles for both systems show a suppressed magnetization that evolves to the bulk value over a length scale of 1-2 nm.

PACS numbers: 75.70.-i, 75.47.Lx

Manganites have been an interesting topic for many years because of the extensive range of dynamic electronic, magnetic, and structural properties they exhibit. Due to strong electron correlations, the manganites have been an area of unexpected physical phenomena such as colossal magneto-resistive behavior associated with both the ferromagnetic (FM) Curie temperature  $T_c$  and the metal-insulator transition [1]. A complex magnetic phase diagram in  $\text{La}_{1-x}\text{A}_x\text{MnO}_3$  evolves with the variation of divalent dopants (i.e.,  $\text{A} = \text{Ba}, \text{Ca}, \text{Sr}$ ), and  $T_c$  can be tuned to well above room temperature [2]. Hole-doped  $\text{La}_{1-x}\text{Sr}_x\text{MnO}_3$  (LSMO) with  $x = 0.3$  is FM and nearly half-metallic at low temperatures. Experiments indicate that the spin polarization of these materials is at least 0.83 [3, 4, 5, 6] (compared with 0.45 for Fe, Ni, Co [4, 5]), with some evidence for it being completely spin polarized [7, 8, 9]. This particular composition of LSMO has been extensively studied, but the properties of the surfaces of films and heterostructures deviate from predictions made from bulk properties alone.

Several groups have investigated magnetic tunnel junctions (MTJs) using manganite films as electrodes and have observed a significant reduction in tunneling magneto-resistance (TMR) between 200 K and 280 K [6, 8, 10, 11]. Spin-resolved photoemission studies by Park et al. [12] indicate that a strong possibility for this loss of TMR is a degraded magnetization at the surface. Recently, an attempt has been made to influence the magnetic properties of an LSMO/SrTiO<sub>3</sub> (STO) interface [13]. Using pulsed laser deposition, 2 unit cells (u.c.) of undoped LaMnO<sub>3</sub> (LMO) were inserted to create an LSMO/LMO/STO structure. Magnetic second-harmonic generation indicated the bulk magnetization is enhanced at the interface, even at room temperature. A direct measurement of the depth-dependent magnetic profile in these materials should lead to a deeper understanding of the mechanisms governing the magnetic properties of thin film manganites and has already led to new insights into the layered manganite compounds [14].

In this letter, we present a measurement of the depth-dependent magnetization profile as a function of temperature across LSMO/STO and modified LSMO/LMO/STO interfaces. The electronic and magnetic structure of the LMO layer introduced at the interface appears to be qualitatively equivalent to the underlying LSMO film. Our results show a FM moment at the LMO/STO interface that is larger than the LSMO/STO interface at low temperature. However, the room temperature magnetic profiles are nearly identical for both interfaces, indicating that reducing the density of doped holes at the interface (i.e., inserting 2 u.c.

of LSMO) does not have a significant effect on the room temperature interface magnetism. At all temperatures, both interfaces show a significantly suppressed interface magnetization that evolves to the bulk value over a length scale of  $\sim 1-2$  nm.

The samples used in our experiment were grown using ozone-assisted atomic layer-by-layer molecular beam epitaxy (AL-MBE) [15] on an STO substrate. The atomic beam fluxes were calibrated to better than 1% accuracy using Rutherford back scattering spectroscopy and x-ray  $\pi$  thickness oscillations on separate films. The growth was carried out at a substrate temperature of 680 C and an ozone pressure of  $2 \times 10^{-6}$  Torr using flux matched co-deposition. Throughout the LSMO growth, RHEED indicated intensity oscillations of the specular reflection characteristic of a 2-dimensional growth mode. X-ray diffraction studies on similar films have shown that the LSMO grows pseudomorphic to the STO substrate. Immediately after the growth of the LSMO layer, one film was capped with 2 u.c. (0.8 nm) of STO (LSMO/STO interface) and the other with 2 u.c. (0.8 nm) of LSMO and 2 u.c. of STO (LSMO/LSMO/STO interface) grown under the same conditions. In previous studies of such single-crystal MTJs comprised of a thin epitaxial  $\text{CaTiO}_3$  or  $\text{SrTiO}_3$  tunnel barrier sandwiched between two  $\text{La}_{0.67}\text{Sr}_{0.33}\text{MnO}_3$  electrodes, large values of TMR exceeding 450% at 15 K were obtained [3, 16]. The structures used to measure the interface magnetization were prepared identically to those MTJs.

To characterize the interface magnetism, two complementary x-ray techniques were used at beam line 4-ID-C of the Advanced Photon Source: x-ray magnetic circular dichroism (XMCD) [17] and x-ray resonant magnetic scattering (XRMS) [18]. Both XMCD and XRMS measurements were taken simultaneously at a fixed incident angle of  $11^\circ$  while varying the temperature over a range of 50 - 300 K using in-plane fields of 500 Oe to saturate the magnetic moment of the sample. The well-established XMCD technique, measured through total electron yield (TEY), probes spin-dependent absorption. It is important to note that the XMCD probes unoccupied states, including both the localized ( $t_{2g}$ ) and de-localized ( $e_g$ ) electrons. Transport measurements, however, only yield information pertaining to the de-localized mobile electron states. Also, the XMCD in the TEY is proportional to an average near-surface magnetic moment because the signal is weighted by an exponential with a decay length (mean free escape depth of electrons emitted from the surface) of  $\sim 1.5$  nm for LSMO.

Analysis of the absorption taken across the Mn  $L_{2,3}$  edges for the two different interfaces have nearly identical line shapes (see Fig. 1a). This indicates the electronic struc-

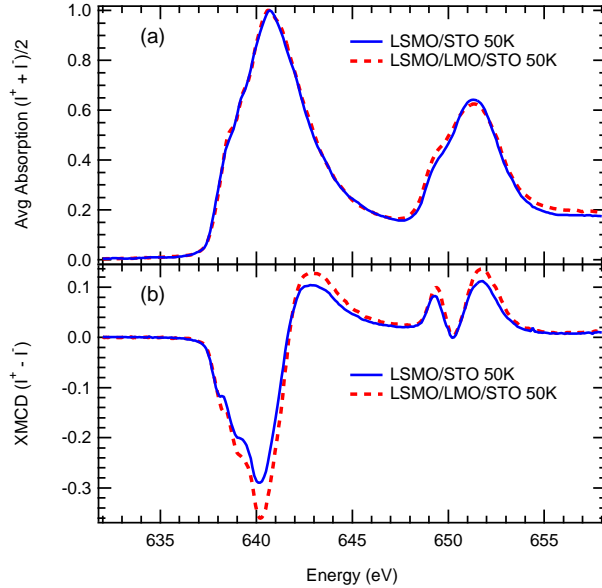


FIG. 1: (Color Online) Top (a): Average absorption across the Mn  $L_{3,2}$  edges showing identical electronic structure for each interface. Bottom (b): The LSMO/LMO/STO interface shows an increase in the near-surface magnetization at low temperature. The identical line shape in the XMCD spectra indicates that the ratio of the spin to orbital moment is the same for each interface.

ture of the unoccupied states in the LMO at the interface is similar to the underlying LSMO. The XMCD shows that the magnitude of the near-surface magnetization for the LSMO/LMO/STO is nearly 10% larger at 50 K (see Fig. 1b). The XMCD line shapes are otherwise identical and can be scaled to overlay exactly, which demonstrates that the ratio of spin to orbital moments is the same. The average magnetization in the surface region is proportional to the area bounded by the XMCD spectra [17]. Due to the identical line shape, the analysis is simplified and the relative magnetization can be described using the maximum peak height. If we plot the XMCD peak height as a function of temperature for each sample and compare with the magnetization measured using SQUID magnetometry [19] of a bulk LSMO single crystal of the same composition ( $x=0.3$ ),  $T_c$ , and transport characteristics, we see that the surface magnetization for each interface is falling off faster than the bulk (see Fig. 2). The average magnetization for the different interfaces shows a similar deviation from the bulk temperature dependence (see Fig. 2).

To construct the shape of the magnetization profile we utilize XRRM, which probes the depth dependence of the magnetization. If we consider an atomic model, the origin

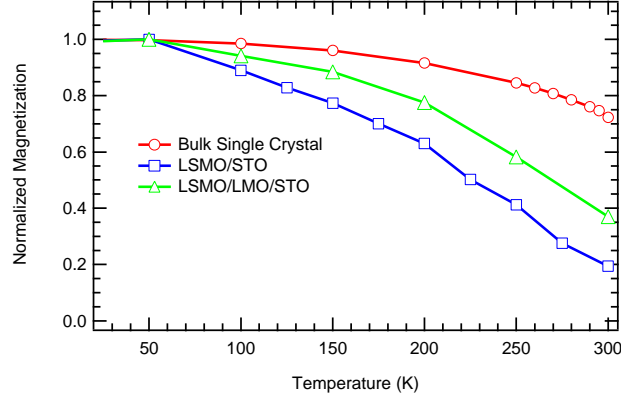


FIG. 2: (Color online) The temperature dependence of the XMCD peak height (proportional to the near-surface magnetization) for the LSMO/STO and the LSMO/LMO/STO interfaces is plotted against the temperature dependence of a bulk single crystal LSMO of the same composition. The LSMO/LMO/STO interface has a slightly better thermal stability than the LSMO/STO interface; however, it is still roughly 40% of the bulk value at room temperature.

of the spin-dependent scattering is due to a spin orbit correction [20]. This term adds a polarization-dependent (right and left circular) charge-magnetic interference term in the scattering amplitude. At the resonant energy of a FM atom, however, this effect is enhanced and the magnetic correction term becomes comparable to the pure charge scattering [18]. The resulting XRM S spectra ( $I^+ - I^-$ ) can be understood as the charge-magnetic correction term in the scattering amplitude where the pure charge scattering has been subtracted off by taking the difference in right and left circular polarization. In the soft x-ray regime, we re-express the distorted-wave Born approximation (DWBA) [21] in a magneto-optical formalism [22]. Then the charge-magnetic term in the scattering amplitude can be interpreted as interference between specularly reflected x-rays from the chemical boundaries and those reflected from magnetic planes.

The quasi-cubic perovskite unit cell contains only one Mn ion, and the distance between possible magnetic scattering planes is fixed by the lattice constant (0.4 nm). Explanation of the XRM S depends on fitting the spectra by varying the average magnetization at each magnetic MnO<sub>2</sub> plane, which is specified by its depth in the sample (i.e., the STO interface being  $z=0$ ). If the incident angle and chemical boundaries are known, the detailed shape of the XRM S depends only on the shape of the magnetization profile. After modeling many magnetic profiles with different functional forms, this methodology has had remarkable suc-

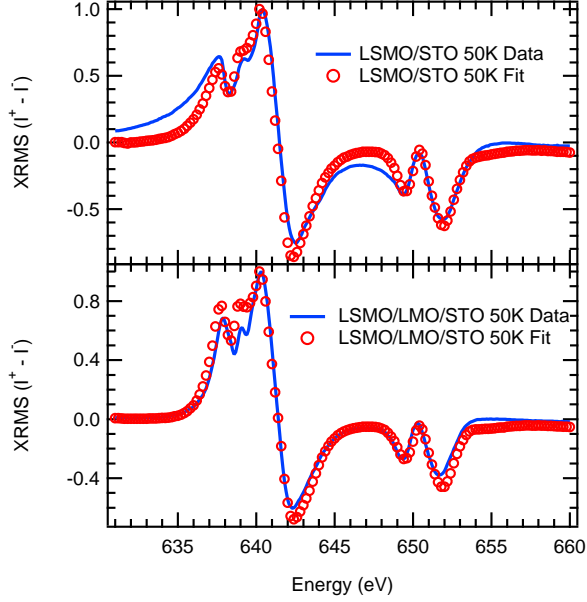


FIG. 3: (Color Online) After modeling many different functional dependencies, the depth-dependent magnetic profiles are presented for both the LSMO/LMO/STO and the LSMO/STO interfaces.  $z=0$  occurs at the STO boundary. The atomically structured interface shows improvement at low temperature; however, the surface magnetization  $M_s = M(z=0)$  is still significantly suppressed.

cess in fitting the observed data (see Fig. 3) and leads directly to the depth-dependent magnetic profile (see Fig. 4). This magnetic profile can now be weighted by the electron escape probability at each temperature to reproduce the results from the near-surface magnetization (XMCD), showing consistency between two independent measurements of the surface magnetism.

The LMO layer in the atomically assembled structure has two main effects on the system. In the LSMO/LMO/STO sample, the surface magnetization ( $M_s = M(z=0)$  defined to be the STO interface) is roughly 70% of the bulk value at low temperatures. At the same time, the low temperature LSMO/STO interface is only 40% of the bulk value. Secondly, the LMO at the interface sharpens the transition region. Each profile demonstrates a continuous decrease from bulk ferromagnetism ( $M=1$ ) to some non-zero value at the interface with a transition region of 1.5 nm (4 u.c.) for the LSMO/LMO/STO interface and 2.5 nm (6 u.c.) for the unmodified interface. In each case though, the length scale set by the transition region is nearly an order of magnitude larger than the Thomas-Fermi screening

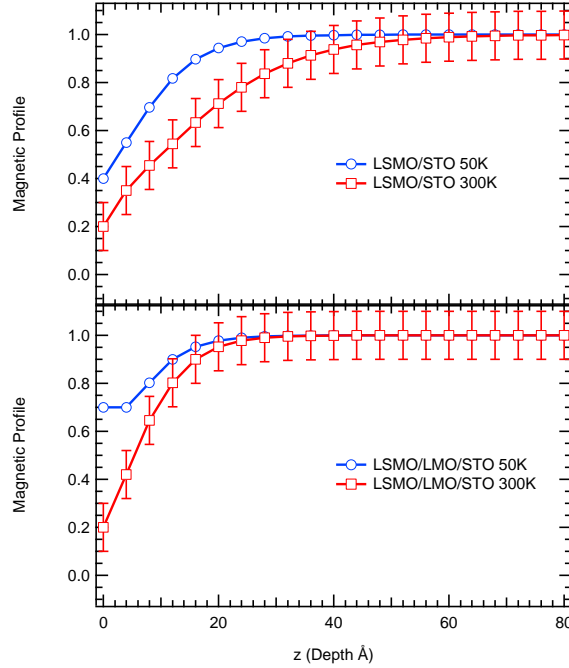


FIG. 4: (Color Online) Data and characteristic fits shown for low-temperature XRM S spectra. Taking the difference in circularly polarized scattering is equivalent to subtracting off the pure charge scattering. The remaining charge-magnetic interference term is modeled. The line shape of the XRM S spectra depends solely on the depth-dependent magnetic profile.

length of  $0.3 \text{ nm}$  predicted from the density of carriers in  $x = 0.3 \text{ LSMO}$  [23]. The XRM S indicates that both the LSMO/STO and LSMO/LMO/STO interfaces have similar magnetic structure. There is a measurable increase in the surface moment outside the experimental error at low temperature, which is also observed in the XMCD (See Fig. 1). At higher temperatures, however, the profiles do not differ more than the experimental error, and each interface converges to approximately the same value of  $M_s$ . The profiles also demonstrate a reversible nature as a function of temperature. Whatever the mechanism for reduction of magnetization at the interface, it appears insensitive to the addition of electrons by the LMO layer.

Additionally, the magnetic profile reveals that the LMO in the LSMO/LMO/STO is FM, whereas bulk LMO is antiferromagnetic (AFM). The average absorption indicates that the electronic structure of unoccupied states is qualitatively the same as the underlying LSMO, suggesting that doped holes can diffuse into the LMO. This places a lower limit on the diffusive length scale of the doped hole carriers of at least  $2 \text{ u.c}$  or  $0.8 \text{ nm}$ . The LMO then

could be effectively doped somewhere in the FM region of the phase diagram. Interdiffusion of Sr atoms into the LMO layer is not likely in these samples because the kinetics of atomic diffusion perpendicular to the surface occur at much higher temperatures than were used in the ALL-MBE growth process. X-ray diffraction and cross-sectional STEM images also do not show any indication of atomic interdiffusion [24].

For a free LSMO surface the reduced magnetization can be attributed to the loss of coordination at the surface resulting in reduced hopping, which will frustrate double exchange and improve the chance of AFM order at the surface. This idea is supported by recent calculations of magnetic surface states of LSMO, which find AFM ordering in the surface layer [25]. Since the XRM S profiles integrate over lateral variations, it is not possible with this measurement alone to determine the lateral variation of the magnetic order at the interface. The surface region could be inhomogeneous, but we show that the surface always has some FM component. One possibility is a percolation behavior in which AFM regions grow as we approach the surface and/or raise the temperature.

The magnetic profile and x-ray spectroscopy both support the idea that the LMO layer is chemically and magnetically similar to the underlying LSMO, suggesting that the doped hole carriers can diffuse over length scales of at least 2 u.c. This is of the same order of magnitude as the transition width of the magnetic profiles across each interface (3 u.c. – 6 u.c). The recent work showing enhanced magnetization at room temperature [13] also reported low-temperature TMR improvement from 50% to 170% (see online supplement ref. 13) compared to a TMR of 45% [3, 16] in high quality LSMO-based tunnel junctions with unmodulated interfaces. At low temperature the magnetization in each system should be saturated and yield similar TMR ratios. The magnetic behavior of the interface, when carefully probed, demonstrates that the smoothly varying surface magnetization is still significantly degraded at all temperatures. Extensive work on the effect of variation of the tunnel barrier in these systems also shows that, in all cases, the temperature dependence of the TMR is similar [16], and from that it can be deduced that the normalized magnetization profiles for various LSMO / tunnel barrier interfaces will be in qualitative agreement with our results.

The use of the Advanced Photon Source was supported by the U.S. Department of Energy, Office of Science, Office of Basic Energy Sciences, under contract W-31-109-ENG-38.

- 
- [1] S. Jin, T. H. T iefel, M .M cCom ack, et al, Science 264, 413 (1994).
- [2] O .Chm aisse, B .D abrowski, S .K olesnik, et al, Phys. Rev. B 67, 094431 (2003).
- [3] J. O 'D onnell, A .E .Andrus, S .O h, et al, Appl. Phys. Lett. 76, 1914 (2000).
- [4] R .J. Soulen, Jr., J. M .B yers, M .S .O sofsky, et al, Science 282, 85 (1998).
- [5] R .J. Soulen, Jr., M .S .O sofsky, B .N adgomy, et al, J. Appl. Phys. 85, 4589 (1998).
- [6] M .V irect, J. N assar, M .D rouet, et al, J. M agn. M agn. M ater. 198-199, 1 (1999).
- [7] J.-H .Park, E .Vescovo, H .-J. K im , et al, Nature 392, 794 (1998).
- [8] M .B owen, M .B ibes, A .B arthelmy, et al, Appl. Phys. Lett. 82, 233 (2003).
- [9] B .N adgomy, I. I. M azin, M .O sofsky, et al, Phys. Rev. B 63, 184433 (2001).
- [10] T .O bata, T .M anako, Y .Shim akawa, and Y .K ubo, Appl. Phys. Lett. 74, 290 (1999).
- [11] C .K won, Q .X .Jia, Y .Fan, et al, Appl. Phys. Lett. 72, 486 (1998).
- [12] J.-H .Park, E .Vescovo, H .-J. K im , et al, Phys. Rev. Lett. 81, 1953 (1998).
- [13] H .Y amada, Y .O gawa, Y .Ishii, et al, Science 305, 646 (2004).
- [14] J. W .Freeland, K .E .G ray, L .O zyuzer, et al, Nature M aterials 4, 62 (2005).
- [15] J. N .Eckstein and I. B ozovic, Annu. Rev. M ater. Sci. 25, 679 (1995).
- [16] V .G arcia, M .B ibes, A .B arthelmy, et al, Phys. Rev. B 69, 052403 (2004).
- [17] C .T .C hen, Y .U .Idzerda, H .-J. L in, et al, Phys. Rev. Lett. 75, 152 (1995).
- [18] C .K ao, J. B .H astings, E .D .Johnson, et al, Phys. Rev. Lett. 65, 373 (1990).
- [19] M .B .Salam on, P rivate C om m unication (2005).
- [20] P .N .A rgyres, Phys. Rev. 97, 334 (1955).
- [21] D .R .Lee, S .K .Sinha, D .H askel, et al, Phys. Rev. B 68, 224409 (2003).
- [22] J. Zak, E .R .M oog, C .Liu, and S .D .Bader, J. M agn. M agn. M ater. 89, 107 (1990).
- [23] X .H ong, A .P osadas, and C .H .A hn, Appl. Phys. Lett. 86, 142501 (2005).
- [24] A .P alanisami, M .P .W arusaw ithana, J. N .Eckstein, et al, Phys. Rev. B 72, 024454 (2005).
- [25] H .Zenia, G .A .G ehling, G .B anach, and W .M .T em m em an, Phys. Rev. B 71, 024416 (2005).